

**CUCKOO SEARCH ALGORITHM-BASED ZETA CONVERTER
IN A PHOTOVOLTAIC SYSTEM UNDER PARTIAL SHADING
CONDITION**

by

JOTHAM JEREMY A/L LOURDES

**Thesis submitted in fulfilment of the requirements
for the degree of
Master of Science**

May 2021

ACKNOWLEDGEMENT

Many people deserve my sincere thanks, but I can only name some of those many people here. If you are one of those many anonymous friends, you will know that I have valued your friendship, love and support during the course of my study. Thank you.

First and foremost, I would like to thank God for His wisdom and knowledge given to me. I dedicate this research to my parents, Mr. and Mrs. Lourdes, and to all my family members for being my backbone by supporting me emotionally, physically, and financially throughout this period.

Furthermore, I express my gratitude and appreciation to my main supervisor Dr. Ooi Chia Ai and co-supervisor Dr. Teh Jiashen for their guidance, motivation and unending support throughout the completion of this research and thesis writing. They have spared a lot of time and energy to help me and provide guidance that I needed to complete this research.

Special acknowledgement goes to the School of Electrical and Electronics Engineering, Universiti Sains Malaysia (USM) for allowing me to conduct the research and supporting me financially for the first year. Moreover, I would like to convey my thanks to the staff in the school for their assistance and cooperation throughout my research progress.

Finally, my deepest gratitude and special thanks go to my closest friends especially Anbalagan and Sanjith for their understandings, moral support, and encouragement. Without the help from the above-mentioned people, it would have been difficult for me to endure the process. May God bless all of us.

TABLE OF CONTENTS

	Page
ACKNOWLEDGEMENT	ii
TABLE OF CONTENTS	iii
LIST OF TABLES	vi
LIST OF FIGURES	vii
LIST OF SYMBOLS	x
LIST OF ABBREVIATIONS	xii
ABSTRAK	xiii
ABSTRACT	xiv
CHAPTER 1 - INTRODUCTION	
1.1 Introduction	1
1.2 Problem Statements	6
1.3 Research Objectives	7
1.4 Significance of Work	7
1.5 Scopes and Limitations	8
1.6 Thesis Outline	9
CHAPTER 2 – LITERATURE REVIEW	
2.1 Introduction	11
2.2 Modelling of Photovoltaic (PV) Panel	11
2.2.1 Single-Diode Model	12
2.3 PV System Installation	13
2.4 Configuration of PV System	15

2.5	Effects of Irradiation and Temperature on PV System	17
2.6	Effects of Partial Shading on PV System	18
2.7	Non-Isolated DC-DC Converter in PV System	19
2.7.1	Buck-boost Converter	21
2.7.2	Cuk Converter	24
2.7.3	SEPIC Converter	26
2.7.4	Zeta Converter	29
2.8	Maximum Power Point Tracker (MPPT) in PV System	31
2.8.1	Conventional MPPT Method	32
2.8.1.1	Modified PO MPPT	35
2.8.2	Artificial Intelligence (AI)-based MPPT Method	35
2.9	Summary	37

CHAPTER 3 - METHODOLOGY

3.1	Introduction	38
3.2	General Simulation Setup of a PV System	38
3.2.1	Choice of resistor	39
3.3	Proposed Integration	40
3.3.1	Zeta Converter	43
3.3.2	Cuckoo Search (CS) Algorithm	48
3.3.2(a)	Fundamental Concept of CS Algorithm	49
3.3.2(b)	Selection of Parameters in CS	53
3.4	Simulation	54
3.4.1	PV Panel	55
3.4.2	Partial Shading Conditions	55

3.5	Measurements & Calculations	59
3.6	Summary	59

CHAPTER 4 – RESULTS AND DISCUSSION

4.1	Introduction	60
4.2	Photovoltaic (PV) Panel	60
	4.2.1 Initialization of Cases	62
	4.2.2 Types of P-V Characteristic Curve	66
4.3	Cuckoo Search (CS) Algorithm as MPPT	68
	4.3.1 Impact of N_{eggs} (solution) in CS MPPT Algorithm	75
	4.3.2 Impact of Zeta converter and CS MPPT Algorithm in PV System	77
4.4	Summary	87

CHAPTER 5 – CONCLUSION AND FUTURE WORK

5.1	Conclusion	88
5.2	Future Works	89

REFERENCES	91
-------------------	----

APPENDICES

Appendix A: Perturb and Observe Algorithm.

Appendix B: Cuckoo Search Algorithm.

LIST OF PUBLICATIONS

LIST OF TABLES

		Page
Table 2.1	Summary of types of DC-DC converters and its characteristics.	20
Table 2.2	Comparisons of MPPTs used in PV system.	36
Table 3.1	Analysis of various resistor value under STC.	39
Table 3.2	Electrical parameters of SunPower SPR-315E-WHT-U PV panel.	41
Table 3.3	Parameters of DC-DC converters.	42
Table 3.4	Irradiance setup of ten (10) evaluation tests on the PV panels (W/m^2).	46
Table 3.5	The converter's P_{conv} efficiency (%) under different irradiance levels (W/m^2).	47
Table 3.6	List of designed cases.	54
Table 3.7	Irradiance setup of four (4) evaluation patterns on the PV panels (W/m^2).	54
Table 4.1	I-V and P-V characteristic curve for Pattern 1.	63
Table 4.2	I-V and P-V characteristic curve for Pattern 2.	64
Table 4.3	I-V and P-V characteristic curve for Pattern 3.	64
Table 4.4	I-V and P-V characteristic curve for Pattern 4.	65
Table 4.5	Simulation results of the proposed integration.	76
Table 4.6	Simulation result for Pattern 1.	82
Table 4.7	Simulation result for Pattern 2.	83
Table 4.8	Simulation result for Pattern 3.	84
Table 4.9	Simulation result for Pattern 4.	85

LIST OF FIGURES

	Page	
Figure 1.1	Global primary energy consumption since year 1800 to year 2019.	2
Figure 1.2	Years of fossil fuel reserves left.	2
Figure 1.3	Basic (a) I-V and (b) P-V curve characteristic of PV module at 25 °C.	4
Figure 1.4	Basic (a) I-V and (b) P-V curve characteristic of PV module at 1000 W/m ² .	5
Figure 2.1	The “knee” point at the I-V and P-V characteristic curve.	12
Figure 2.2	Single diode model for PV system.	12
Figure 2.3	Block diagram of a stand-alone PV system.	14
Figure 2.4	Block diagram of a grid-connected PV system.	14
Figure 2.5	PV panel configuration in (a) series and (b) parallel.	15
Figure 2.6	The individual and sum values of (a) V_{out} , (c) I_{out} , (e) P_{out} of PV panel in series, and (b) the V_{out} , (d) I_{out} , (f) P_{out} of PV panel in parallel under identical PSC.	16
Figure 2.7	Basic model of a DC-DC converter.	21
Figure 2.8	Circuit configuration of buck-boost converter.	22
Figure 2.9	Circuit configuration of Ćuk converter.	25
Figure 2.10	Circuit configuration of SEPIC converter.	27
Figure 2.11	Circuit configuration of Zeta converter.	29
Figure 2.12	Flowchart of PO MPPT algorithm.	33
Figure 2.13	Flowchart of INC MPPT algorithm.	34
Figure 3.1	General block diagram of a PV system.	39

Figure 3.2	Series-connected PV panel.	42
Figure 3.3	Implementation of the PV system in MATLAB Simulink.	43
Figure 3.4	Circuit connection of Zeta converter.	44
Figure 3.5	Zeta converter operation in ON state.	45
Figure 3.6	Zeta converter operation in OFF state.	45
Figure 3.7	The P_{conv} efficiency (%) of each converter under different irradiance levels.	48
Figure 3.8	Flowchart of CS MPPT algorithm.	50
Figure 3.9	The pseudo code for CS algorithm	52
Figure 3.10	Single PV panel connection.	55
Figure 3.11	The complexity of the P-V characteristic curve reflecting the various types of PSC pattern based on Table 3.7; i.e. (a) Pattern 1, (b) Pattern 2, (c) Pattern 3, (d) Pattern 4.	58
Figure 4.1	(a) I-V and (b) P-V characteristic curve of single SunPower SPR-315E-WHT-U under different weather conditions at 25 °C.	61
Figure 4.2	I-V and P-V characteristic curve of single and three SunPower SPR-315E-WHT-U PV panel at irradiance level of 1000 W/m ² and temperature at 25 °C.	62
Figure 4.3	P-V characteristic curve complexity subject to different PSC patterns.	68
Figure 4.4	The MPP searching mechanism by CS MPPT algorithm with $N_{eggs} = 3$ subject to PSC Pattern 4.	69
Figure 4.5	Response of egg position in CS MPPT algorithm with $N_{eggs} = 3$ and its respective V_{in} .	71

Figure 4.6	Response of egg position in CS MPPT algorithm with $N_{\text{eggs}} = 3$ and its respective P_{in} .	71
Figure 4.7	The MPP searching mechanism by CS MPPT algorithm with $N_{\text{eggs}} = 4$ subject to PSC Pattern 4.	72
Figure 4.8	Response of egg position in CS MPPT algorithm with $N_{\text{eggs}} = 4$ and its respective V_{in} .	74
Figure 4.9	Response of egg position in CS MPPT algorithm with $N_{\text{eggs}} = 4$ and its respective P_{in} .	74
Figure 4.10	The tracking movement of PO MPPT algorithm in Pattern 1.	78
Figure 4.11	The tracking movement of PO MPPT algorithm in Pattern 2.	78
Figure 4.12	The tracking movement of PO MPPT algorithm in Pattern 3.	79
Figure 4.13	The tracking movement of PO MPPT algorithm in Pattern 4.	80
Figure 4.14	(a) P_{in} efficiency, (b) P_{out} efficiency, (c) P_{conv} efficiency (d) P_{in} oscillation, (e) P_{out} oscillation of the converters and (f) t_s subjected to Pattern 1.	82
Figure 4.15	(a) P_{in} efficiency, (b) P_{out} efficiency, (c) P_{conv} efficiency (d) P_{in} oscillation, (e) P_{out} oscillation of the converters and (f) t_s subjected to Pattern 2.	83
Figure 4.16	(a) P_{in} efficiency, (b) P_{out} efficiency, (c) P_{conv} efficiency (d) P_{in} oscillation, (e) P_{out} oscillation of the converters and (f) t_s subjected to Pattern 3.	84
Figure 4.17	(a) P_{in} efficiency, (b) P_{out} efficiency, (c) P_{conv} efficiency (d) P_{in} oscillation, (e) P_{out} oscillation of the converters and (f) t_s subjected to Pattern 4.	85

LIST OF SYMBOLS

Symbols	Description
%	Percentage
\otimes	Multiplication
i	Sample number
I	Current
I_{in}	Input current
I_{LMPP1}	Current at local maximum power point 1
I_{LMPP2}	Current at local maximum power point 2
I_{mpp}	Current at maximum power point
I_{out}	Output current
I_{pv}	Photovoltaic current
I_{sc}	Short circuit current
k_i	Factor of ratio
n	Nest size
N_{cell}	Cells per module
N_{eggs}	Number of eggs
N_p	Number of parallel connected PV cells
N_s	Number of series connected PV cells
$^{\circ}C$	Temperature
P	Power
P_a	Probability of the host bird finding out the cuckoo egg
P_{conv}	Power conversion
P_{in}	Input power
P_{LMPP1}	Power at local maximum power point 1

P_{LMPP2}	Power at local maximum power point 2
P_{losses}	Power losses in the converter
P_{MPP}	Power at maximum power point
P_{out}	Output power
P_{pv}	Photovoltaic power
R_{in}	Input impedance
R_{out}	Output impedance
s	Time in seconds
t	Iteration number
t_s	Settling time
V	Voltage
V_{in}	Input voltage
v_i^t	Samples/eggs (N_{eggs})
V_{LMPP1}	Voltage at local maximum power point 1
V_{LMPP2}	Voltage at local maximum power point 2
V_{mpp}	Voltage at maximum power point
V_{oc}	Open circuit voltage
V_{out}	Output voltage
V_{pv}	Photovoltaic voltage
W/m^2	Irradiance level
α	Step size
γ	Gamma function
ΔP	Changes in power
ΔV	Changes in voltage
θ^*	Cell temperature reference

LIST OF ABBREVIATIONS

Abbreviation	Description
AI	Artificial Intelligence
CCM	Continuous conduction mode
CS	Cuckoo search
D	Duty cycle
FLC	Fuzzy logic control
HID	High-intensity discharge
INC	Incremental conductance
I-V	Current-Voltage
LMPP	Local maximum power point
MaxIt	Maximum iteration
MP	Maximum power
MPP	Maximum power point
MPPT	Maximum power point tracker
N	Number of the series-connected PV cells
PO	Perturb and observe
PSC	Partial shading condition
PV	Photovoltaic
P-V	Power-voltage
PWM	Pulse width modulation
RESs	Renewable energy sources
SS	Steady-state
STC	Standard test conditions
TAB	Triple active bridge

ALGORITMA PENCARIAN 'CUCKOO' BAGI PENUKAR 'ZETA' DALAM SISTEM FOTOVOLTAIK DIBAWAH KEADAAN SEPARA TEDUH

ABSTRAK

Isu utama algoritma pengesanan titik kuasa maksimum konvensional adalah kekurangan kecekapan sistem dalam situasi separa berlorek yang disebabkan oleh kehadiran titik maksima yang lebih rendah pada lengkung kuasa-voltan. Tesis ini mencadangkan integrasi baru pencarian algoritma Cuckoo dan penukar kuasa Zeta dalam sistem fotovoltaik di mana ia meningkatkan kecekapan kuasa pengeluaran dan mengurangkan masa pengesanan kuasa maksimum, serta pengurangan riak pengeluaran. Untuk mengesahkan keberkesanan integrasi baru ini, pencarian algoritma Cuckoo dibina dalam MATLAB simulink menggunakan penukar kuasa Zeta. Dengan penggunaan penukar kuasa Zeta, keluaran riak kuasa pengeluaran telah dikurangkan sebanyak 2.92 %. Justeru, kecekapan kuasa keluaran diperbaiki sebanyak 1.25 %. Masa pengesanan kuasa maksimum telah dikurangkan sebanyak 14 % berbanding dengan penukar kuasa buck-boost. Di samping itu, kesan penggunaan lebih banyak telur (solusi) dalam algoritma carian Cuckoo juga dikaji untuk kedua-dua penukar kuasa “Zeta” dan “Buck-boost” untuk mengenalpasti kesannya ke atas ketepatan pengesanan titik kuasa maksimum. Pada Corak 4, penarafan kuasa maksimum untuk keluaran fotovoltaik dalam tesis ini ialah 523.97 W. Integrasi baru ini berjaya mendapat kuasa masukan 523.4 W dan kuasa keluaran sebanyak 493.2 W, masing-masing sebanyak 99.89 % dan 94.13 % daripada kuasa maksimum. Di bawah integrasi konvensional, sistem ini hanya mendapat kuasa masukan 516.0 W dan kuasa keluaran 469.1 W, iaitu 98.47 % dan 89.52 % dari kuasa maksimum.

CUCKOO SEARCH ALGORITHM-BASED ZETA CONVERTER IN A PHOTOVOLTAIC SYSTEM UNDER PARTIAL SHADING CONDITION

ABSTRACT

The key issue with the conventional maximum power point tracking algorithms is the system efficiency in partial shaded conditions due to the presence of local maxima points on the power-voltage curve. This thesis proposes a new integration of Cuckoo Search maximum power point tracking algorithm and Zeta converter in a photovoltaic system where it highlights an improvement of output power efficiency and maximum power point tracking time, as well as reduction of output power ripple. To validate the effectiveness of the work, a Cuckoo Search maximum power point tracking model was constructed in MATLAB Simulink using various irradiance patterns for Zeta converter. In Zeta converter, the output power ripple has been reduced by 2.92 %, thus improving the output power efficiency by 1.25 %. The maximum power point tracking time has been reduced by 14 % compared to that in buck-boost. In addition, the effect of having more eggs (solution) in the Cuckoo Search algorithm was also investigated for both Zeta and Buck-boost converters to study its impact on the maximum power point tracking accuracy. At Pattern 4, the maximum output power of the photovoltaic system in this work is 523.97 W. The proposed integration is able to gain input power 523.4 W and output power of 493.2 W, which are 99.89 % and 94.13 % of the maximum power respectively. With conventional integration, the system is only able to gain 516.0 W input power and 469.1 W output power, which are 98.47 % and 89.52 % of maximum power.

CHAPTER ONE

INTRODUCTION

1.1 Introduction

Energy is a key element in this world's social, economic and technological development. Energy has also been a fundamental human need and its worldwide demand is increasing rapidly due to the expanding energy utilization. The increase in consumption is mainly due to the expansion of industrialization. This has been a prime concern for users due to the lack of resources to meet the energy demand.

In the past years, the primary source of energy comes from the fossil fuel [1]. Figure 1.1 shows the global primary energy consumption since year 1800 to year 2019. In year 2019, the consumption has multiplied almost five times than the consumption in year 1950 which shows the demand of energy. Natural gas, crude oil and coal are the main three source of energy. Renewable energy sources (RESs) only contributes to a tiny percentage of the energy supply. Figure 1.2 shows the fossil fuel (coal, natural gas and oil) reserves left for consumption. It can be observed that in a century to come, the fossil fuel supply will be totally depleted, thus, it is important that the primary source of energy be shifted to RESs. The depletion of fossil fuels and other unfriendly effects on the earth has caused concern for all. Moreover, the use of fossil fuels as the primary source of energy has led to climate change and environmental pollution. Other energy issues like energy imports, rising energy cost and energy inefficiency have also been equally important issues that need to be combated. Thus, it is necessary to look for an alternative energy resource that could supply the demand without harming the earth.

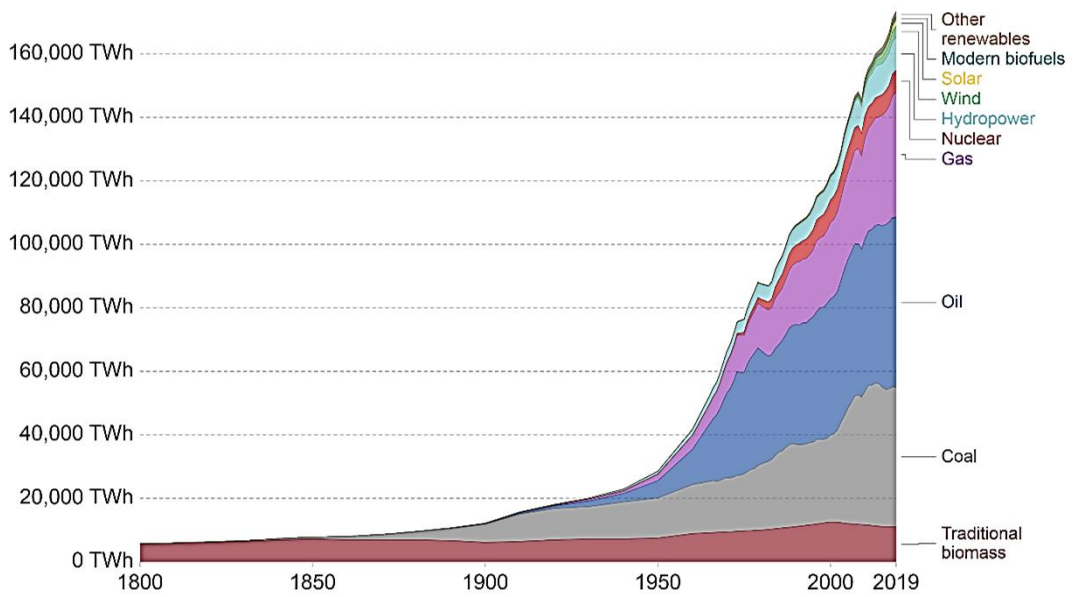


Figure 1.1 Global primary energy consumption since year 1800 to year 2019 [1].

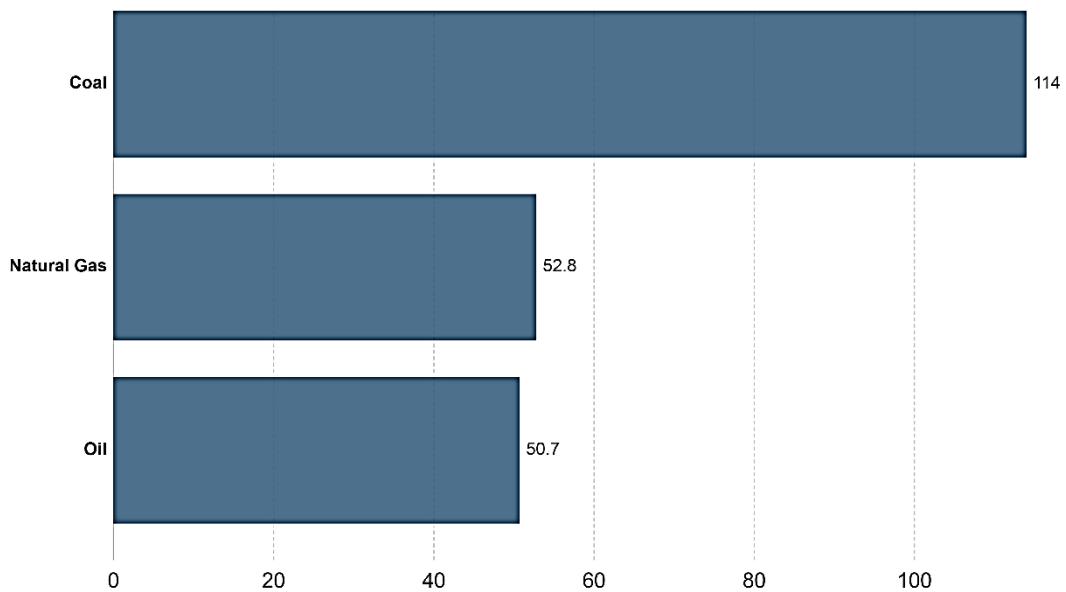


Figure 1.2 Years of fossil fuel reserves left [1].

Extensive research has been performed on RESs, particularly in solar, wind, biomass, geothermal and hydro, to find a good and non-depleting energy supply. It is recognized and accepted that in the future these RESs will play crucial role as they are easy to use, environmentally sustainable and clean energy. Solar energy currently gathers more interest among these RESs choices because it does not contribute to any

kind of carbon emissions or pollution, such as noise, air, or water pollution. The only emissions associated with solar energy are from the production of the materials and components. Furthermore, the energy source comes directly from sunlight, and no human interference is needed. It has become popular among researchers and users over the last decade because of these advantages [2].

Photovoltaic (PV) system is used to convert solar energy that comes from the sun in the form of solar irradiance, into electricity. PV system can be either a stand-alone or a grid-connected generating unit. A stand-alone PV system is used in rural areas where the grid availability is limited. They are manufactured to withstand harsh weather conditions such as high temperatures, humidity in the atmosphere or acidity in the rain. Furthermore, PV systems come with variety of sizes and output for different applications. They are also lightweight, easy to transport. A PV panel contains PV cells that are semiconductors, which absorbs and converts the solar energy into the electrical energy.

Efficiency is an important aspect that needs to be considered in developing a PV system. System reliability can be improved when the efficiency of the system is improved. PV module's conversion performance is comparatively poor therefore finding maximum power point (MPP) is crucial to extract the maximum power (MP) in PV system. When a PV module and load are paired, a mismatch between PV module and load prevents the system from working at its MPP. The load operating point is found at the current-voltage (I-V) characteristic curve knee as displayed in Figure 1.3. This shows the non-linear characteristics of PV module. In addition, the MPP depends on the surrounding weather conditions such as irradiance from the solar and cell temperature. This makes the tracking complicated and not straight-

forward. Changes in irradiation and temperature cause the output power (P_{out}) to be inconsistent and low in efficiency [3-6].

Figure 1.3 also shows the change in MPP on the power-voltage (P-V) curve with change in irradiance at constant temperature, i.e. 25 °C. As the irradiance increases, the P_{out} also increases.

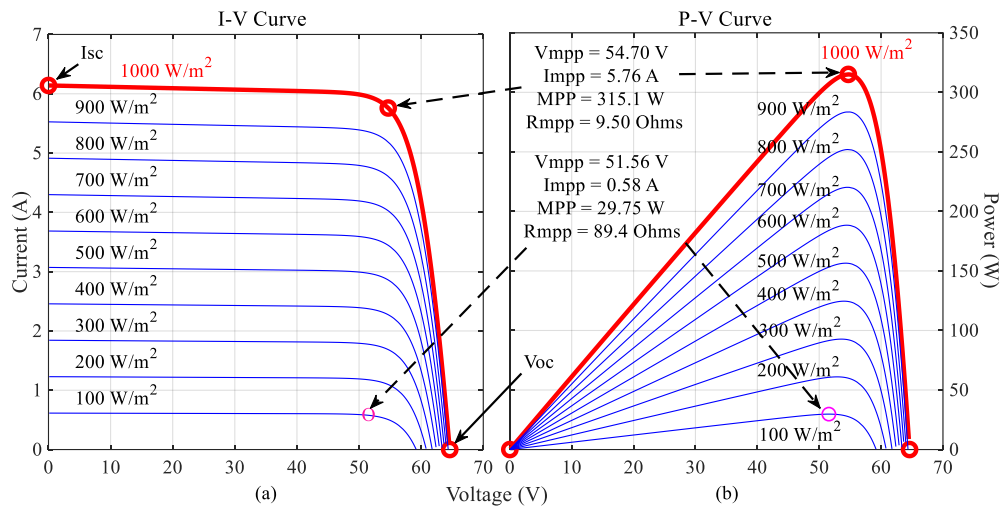


Figure 1.3 Basic (a) I-V and (b) P-V curve characteristic of PV module at 25 °C.

Figure 1.4 shows the change in MPP on the P-V curve corresponding to the change in module temperature at a constant irradiance, i.e. 1000 W/m². As the temperature increases, the P_{out} decreases. Unfortunately, an increase in solar irradiance results in an increase in module temperature, making it even more challenging to the track MPP. Furthermore, when several different modules do not receive the same level of irradiation, the tracking becomes inefficient, this condition is called partial shading condition (PSC).

Usually, a power conditioner such as a DC-DC converter is used as an interface between the PV module and the load to solve the problems described above. Often, MPP tracker (MPPT) is applied together to control the converter's duty cycle (D), which allows the PV module to work at its MPP. MPPT is an algorithm

that works between a PV module and a DC-DC converter [7-9]. The efficiency of the PV system is affected by three factors, namely the efficiency of PV panel, the efficiency of the converter and the efficiency of the MPPT.

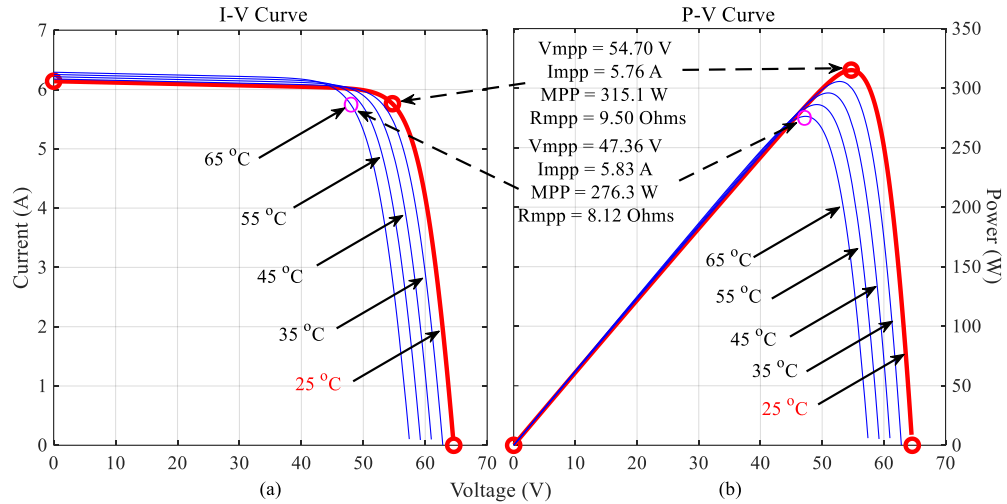


Figure 1.4 Basic (a) I-V and (b) P-V curve characteristic of PV module at 1000 W/m^2 .

Various types of MPPT algorithms have been developed in recent years. They differ in terms of complexity, implementation, sensors requirement, accuracy, costs, efficiency, etc. One of the most important factors in evaluating the MPPTs is the ability to respond to PSC. Conventional MPPTs like perturb and observe (PO) and incremental conductance (INC) algorithms fail to detect the MPP when there is PSC on PV module. PSC is a condition in which the irradiation PV modules are not consistent or in which the panels are partially shaded. Here, there are chances that these MPPTs tracks one of the local MPPs instead of the global MPP [5]. On top of that, the oscillation around the MPP causes fluctuation at the steady-state (SS) response, resulting in long-term power loss and energy dissipation [10]. Also, extensive research has been conducted recently and artificial intelligence-based MPPT methods have been introduced to track MPPs accurately. In this thesis, Cuckoo Search (CS) algorithm MPPT is proposed to overcome this drawback.

1.2 Problem Statements

Solar energy is a continuous source of energy. Despite being free and abundant, the energy generating system, i.e. PV system has two major problems. The energy conversion efficiency is low, especially under low irradiance. Secondly, the generated power is extremely dependent on surrounding conditions, i.e. temperature and irradiance as well as other factors such as the angle of PV panel inclination, aging of PV panels and load condition [3-6].

To increase the output efficiency of PV system, MPPT is introduced. Up to this date, numerous MPPT techniques have been designed to aid the tracking of maximum power point in PV system. MPPT searches for the best working point in the P-V characteristic curve at a given surrounding condition. PO is the most common and preferred MPPT due to its simplicity. It uses power and voltage as the control variable. The algorithm tracks MPP by perturbing the operating point based on the previous increment. If the power increases, the perturbation remains in the same direction, if the power decreases, the perturbation changes to the opposite direction. The drawback of the algorithm is the high oscillation produced at the MPP causing high power loss and energy dissipation. Larger perturbation would increase the tracking speed, but would cause high oscillation, whereas smaller perturbation lowers down the oscillation but the tracking time would increase [8,11,12].

Another problem with PV system is the PSC. In this condition, the PV cells experience different irradiance levels, causing the shaded panel to become reverse biased with high resistance. This produces multiple peaks in the P-V curve depending on the number of bypass diodes in PV cell [5]. PO algorithm does not track well in this condition as the tracking will get trapped at one of the lower points causing lower output power [10].

This thesis will develop an integration to overcome these issues mentioned above and the model can be used in future extended studies.

1.3 Research Objectives

The main objective of this work is to propose the integration of the CS algorithm, an MPPT controller on the DC-DC Zeta converter that tracks the MPP under the standard and PSC on PV module. The proposed method improves the P_{out} efficiency, reduces the P_{out} ripple and reduces the settling time (increased tracking speed). To achieve this aim, the specific objectives are listed below:

- i. To propose an artificial intelligence (AI)-based MPPT in a PV system.
- ii. To integrate CS algorithm and Zeta converter to track MPPT.
- iii. To evaluate the performance of the integration in terms of P_{out} efficiency, output ripple and tracking speed.

1.4 Significance of Work

In this work, a new integration of CS algorithm and Zeta converter to track the MPP under PSC is introduced. P_{out} efficiency, P_{out} ripple and tracking speed are three crucial elements that determine a quality of PV system. The Zeta converter possess a nature where its P_{out} ripple is lower than most of the converters available. Integrating a Zeta converter in PV system reduces the ripple at the output side which improves the PV system's stability. Furthermore, CS MPPT algorithm is able to track MPP efficiently under PSCs, which increases the tracking accuracy and MP harvest. The findings were contrasted with the simulation of these three other cases that are a) integration of PO and Zeta converter, b) integration of CS algorithm and

buck-boost converter and c) integration of PO and buck-boost converter. The main contributions of this work are as the following:

- i. Lower P_{out} ripple was observed in the proposed PV system in comparison to PV system that uses buck-boost converter.
- ii. Higher accuracy in MPP tracking is shown by CS MPPT algorithm in the proposed PV system in comparison to PV system that uses PO MPPT algorithm.
- iii. The effect of different N_{eggs} on the P_{out} is observed to be minimum due to the lower number of PV panel used in this PV system.

1.5 Scopes and Limitations

This thesis aims to design and simulate the integration of CS MPPT algorithm and Zeta converter which works well under PSC in a PV system. A MATLAB Simulink model of PV system with Zeta converter and CS algorithm is built and is verified in order to maximize the generated P_{out} from PC system. A specific single poly-crystalline PV cell is used as the PV source. The system is simulated and tested for four PSC patterns. The Pattern 1 occurs when there is no shading. The Pattern 2 and Pattern 3 occur when one of the panels is shaded. The difference between Pattern 2 and Pattern 3 is the difference in the irradiance intensity on the shaded panel which causes the P-V curve to be different from each other. The Pattern 4 occurs when all three panels receive different irradiance levels. It is important to know the behaviour of the MPP tracking for each type of pattern, hence the reason why simulation is conducted in four different types of PSC. Further explanation in this matter is discussed in Section 4.2.2. Although the design of the

controller in this work is independent of the load, a resistive load of 30Ω is used for simulation. The reason behind the selection of 30Ω is given in Section 3.2.

1.6 Thesis Outline

This thesis is categorized into five main chapters which are the introduction, literature review, methodology, results and discussion, and finally conclusion and future work.

Chapter 2 describes an overview of the existing work on renewable energy, solar energy and the operation of PV systems, including the configuration and arrangements of PV panel. The surrounding weather influence and PSC effects are also discussed. Thereafter, a review on a four non-isolated buck-boost derived DC–DC converters will be presented, i.e. buck-boost, \acute{C} uk, SEPIC and Zeta converter, particularly in the scope of PV applications, the operating modes and equations of the converter will be presented. Finally, few MPPT control techniques that commonly used for PV system are explained and reviewed namely Perturb and Observe, Incremental Conductance, Fuzzy Logic Control (FLC), Neural Network, Ant-Colony Optimization and Cuckoo Search Algorithm. In the end, a brief summary will be presented at the end of this chapter.

Chapter 3 presents methodology of this research which contains two essential components: modelling the new integration in MATLAB Simulink and comparing it to the other integration cases. Initially, the design of the Zeta converter and Cuckoo Search Algorithm is discussed, the simulation-based model of the proposed integration will be designed, illustrated and examined. Next, the other integrations will also be simulated to verify and judge the proposed integration.

Chapter 4 clarifies the analysis of simulation results of the proposed integration for a PV system. Data are taken, organized and presented in tables, graphs, figures and diagrams in a manner that visualizes the significance of certain variables better and to aid the interpretation of the whole research. A comparison is made between the results obtained from the proposed method and the other integrations, i.e. Zeta converter and PO algorithm, buck-boost converter and CS algorithm, and buck-boost and PO algorithm in three aspects, i.e. P_{out} efficiency, P_{out} ripple and time taken to reach SS.

Finally, in Chapter 5, the thesis is concluded. It comprises the conclusion of achieving the objectives outlined in this thesis. It also highlights the contribution of this work and the summarized discussion. The recommendation for future works will also be laid out in this chapter. The references and appendices are attached at the end of the thesis.

CHAPTER TWO

LITERATURE REVIEW

2.1 Introduction

This chapter reviews the existing works on PV system. It comprises of the PV panel in general, its installation and configuration. Then, a review on existing DC-DC converters and maximum power (MP) point (MPP) trackers (MPPTs) are given.

2.2 Modelling of Photovoltaic (PV) Panel

A PV cell is the building block of a PV array. A PV module is formed by connecting numerous PV cells in series and parallel. Several PV modules are connected in series and parallel to form a PV panel. By connecting several PV panels in series and parallel, a PV array is formed.

There are three key parameters in a PV system. These include short circuit current (I_{sc}), open circuit voltage (V_{oc}) and MPP. The power produced at I_{sc} and V_{oc} is zero. The MP is achieved within the I_{sc} and V_{oc} points. The current and voltage at MPP are defined as I_{mpp} and voltage at V_{mpp} respectively. The I_{mpp} , V_{mpp} and the power correspond to a particular load resistance that can be found by Ohm's Law. A unique point can be observed at P-V characteristic curve's "knee", and this is the MPP at which the PV cell generates the MP. The position of the "knee" of the P-V curve is at the intersection point of the dotted vertical and dotted horizontal line as shown in Figure 2.1 [13].

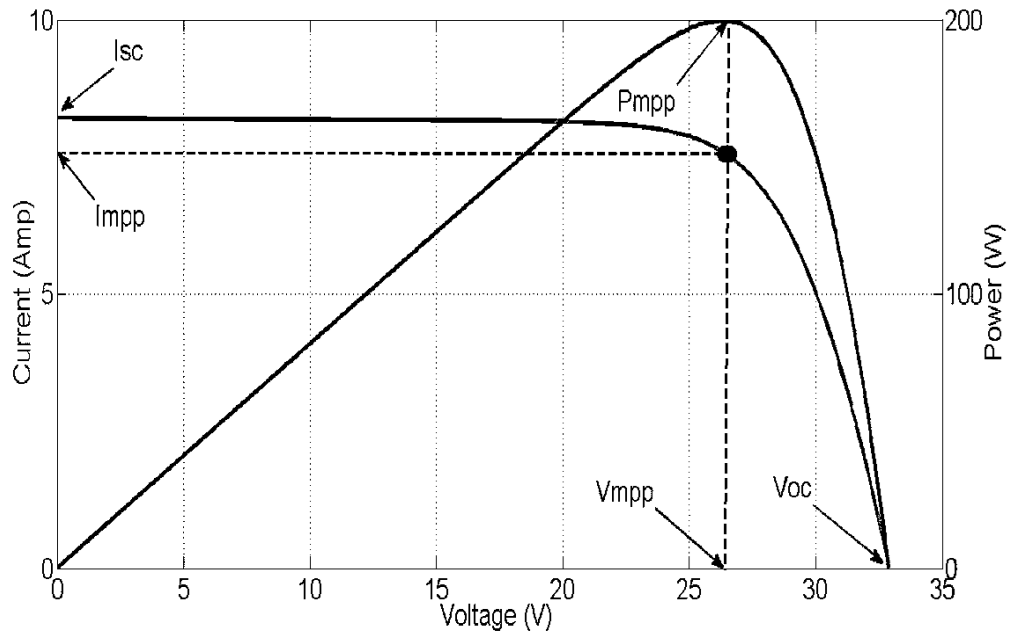


Figure 2.1 The “knee” point at the I-V and P-V characteristic curve [13].

2.2.1 Single-diode model

PV cells can be represented in an equivalent electrical circuit called single-diode model. This single diode model consists of a photosensitive current source, a diode, parallel and series resistors as shown in Figure 2.2.

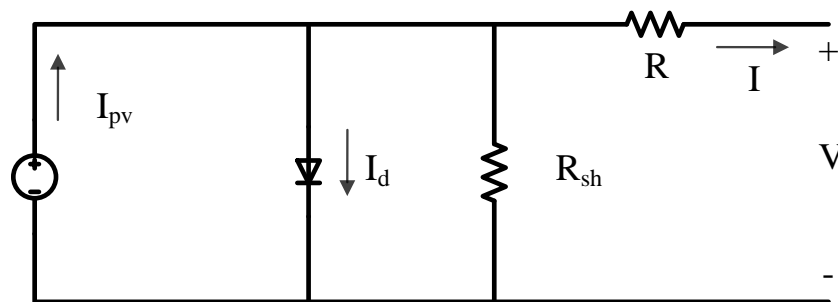


Figure 2.2 Single diode model for PV system.

Using this circuit, the current output of PV cell can be expressed as

$$I = I_{pv} - I_d - \frac{V + RI}{R_{sh}} \quad (2.1)$$

Where I_{pv} is the current generated by the light incidence, I_d can be shown in more detail by Shockley's diode equation and summarized as below.

$$I = I_{pv} - I_0 \left[\exp \frac{q(V + RI)}{nkT} - 1 \right] - \frac{V + RI}{R_{sh}} \quad (2.2)$$

Where I_0 is the reverse saturation current; q is the electron charge; n is the ideality factor of the diode; k is the Boltzmann constant; T is the temperature in Kelvin of the p-n junction. Thermal voltage is defined as

$$V_t = \frac{kT}{q} \quad (2.3)$$

When the PV system is connected in series, the terminal voltage increases, whereas parallel connection increases the output current. Thus, the single-diode model can be simplified as

$$I = I_{pv} - I_0 \left[\exp \frac{(V + RI)}{nN_s V_t} - 1 \right] - \frac{V + RI}{R_{sh}} \quad (2.4)$$

Where N_s is the number of cells in series, I_{pv} and I_0 are determined by cells in parallel. R is the equivalent series resistance which is the losses in electrodes, semiconductors and contact in between these. R_{sh} is the equivalent parallel resistance which represents the losses in the p-n junction. Typically, R is low and R_{sh} is high.

2.3 PV System Installation

There are two major installation types of PV systems: stand-alone and grid-connected systems.

A stand-alone system shown in Figure 2.3 is equally known as the off-grid system, is economical for remote and isolated areas where the source of the grid is limited, provided that enough sunlight is available. It consists of a PV panel, a converter or inverter, and a battery that stores excess energy. The principles of

operation for stand-alone PV system is, it generates power during the day and stores excess energy in battery then supply power through the battery during the night [14].

In a grid-connected system shown in Figure 2.4, the PV system is connected to the power line. This system can supply a large amount of electrical power and can be stored to be sold to the utility. For grid-connected systems, the PV panel output is fed directly to the grid. Since the output of PV cells is DC, it must be converted to AC by using an inverter so that it can be connected to the grid.

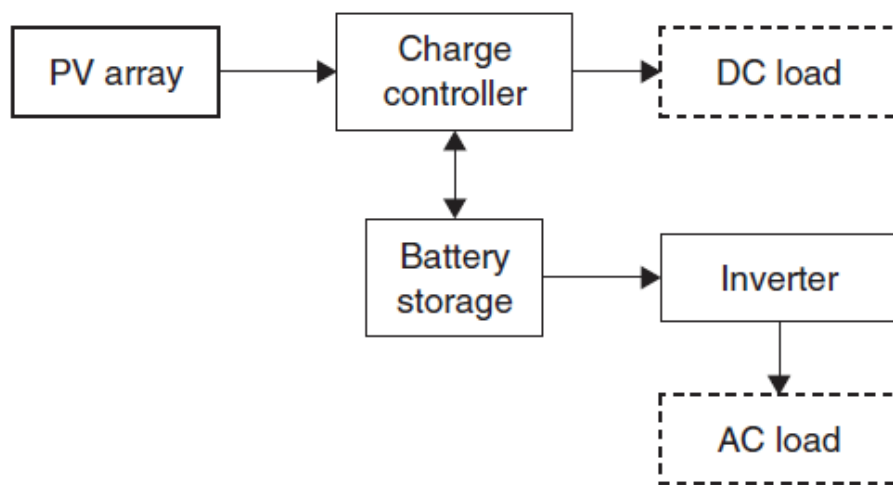


Figure 2.3 Block diagram of a stand-alone PV system [14].

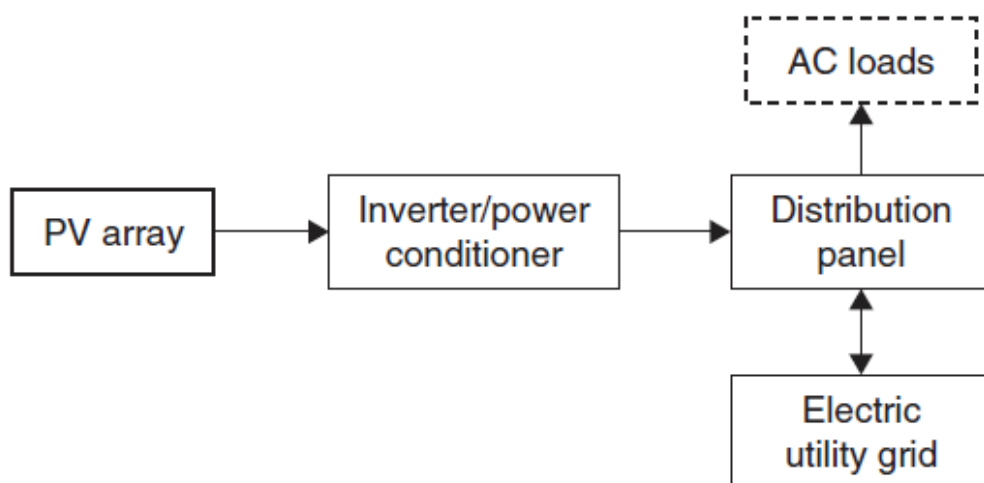


Figure 2.4 Block diagram of a grid-connected PV system [14].

2.4 Configuration of PV System

The power demand is not satisfied with one PV cell as the P_{out} of a single PV cell is not adequate. It is therefore important to connect the modules either in a series, a parallel connection or a combination of both. Figure 2.5 (a) and (b) shows the series and parallel PV cell connection respectively. Connection in series increases the voltage and parallel connection increases the current. The selection of configuration depends on the V_{out} , I_{out} and P_{out} needed to supply the load or a power converter. A PV module is a group of several PV cells that are electrically connected by series and/or parallel circuits to produce the necessary current and voltage. The characteristic of the PV module is based on the number of series (N_s) and parallel (N_p) connected PV cells [15].

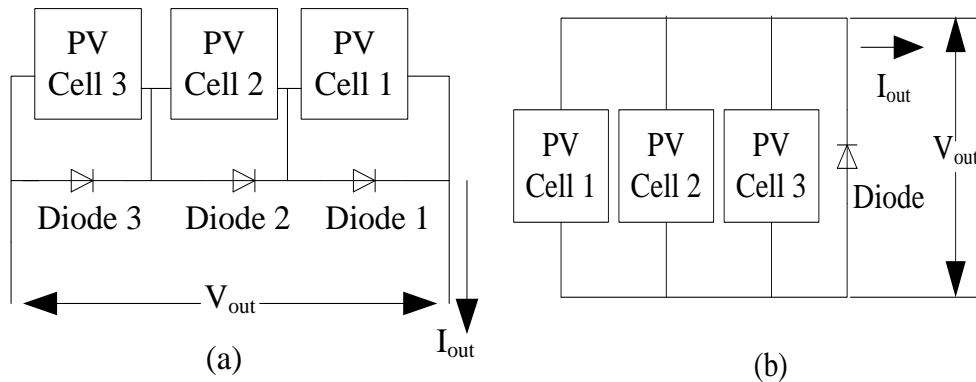


Figure 2.5 PV panel configuration in (a) series and (b) parallel.

When the panels get shaded with different partial shading condition (PSC) (the condition will be further explained in Section 2.6), the attainable P_{max} from PV panel are unequal for series and parallel configuration. This can be seen from Figure 2.6 where all output values are different for series and parallel. The series configured PV panel has multiple power peaks due to the presence of bypass diode in parallel across the PV cell. The bypass diode is required to avoid the reverse flow of current

due to voltage mismatch. This is not effective in the parallel shading because current is able to pass through the unshaded parallel PV cells with lower resistance and neglect the pathway of shaded cells [16,17].

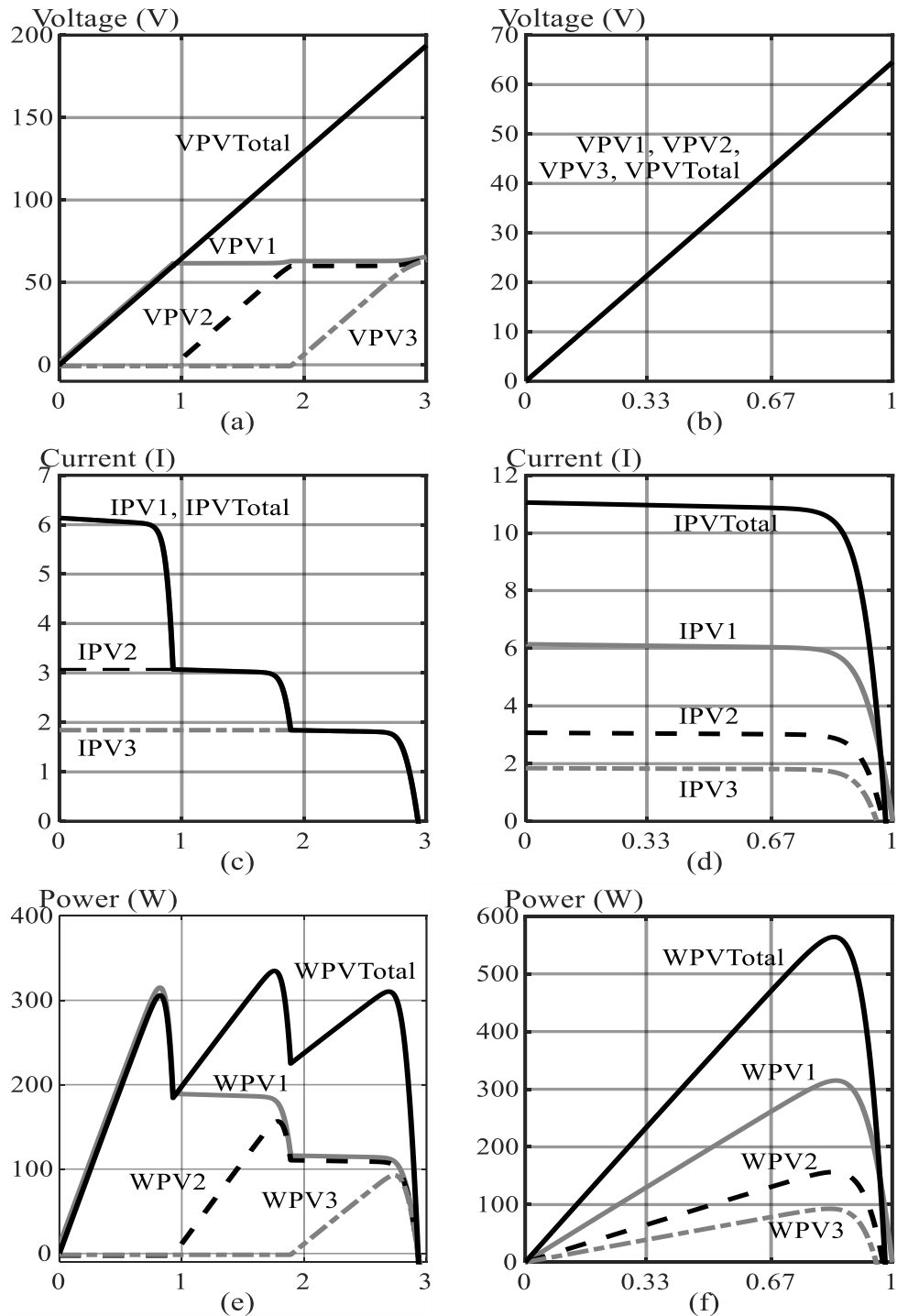


Figure 2.6 Individual and sum values of (a) V_{out} , (c) I_{out} , (e) P_{out} of PV panel in series, and (b) the V_{out} , (d) I_{out} , (f) P_{out} of PV panel in parallel under identical PSC.

In addition, in series connection, the V_{out} generated is higher than parallel connected PV panel. Conversely, the I_{out} produced for series configuration is lower than the parallel configuration for the identical shading pattern. Since this thesis focuses on the tracking of MPPT in PSC, a series connected PV system had to be used as it will produce multiple peaks in P-V characteristic curve.

2.5 Effects of Irradiation and Temperature on PV System

Two crucial factors play important role on the PV output. They are the solar irradiation and temperature on the PV module. Temperature and irradiation are atmospheric condition which can change due to the presence of clouds and the different sunlight ray angle. They have a strong impact on the PV output. The P_{out} from PV panel is proportionate to the solar irradiance but inversely proportionate to the temperature. Since the irradiation and temperature constantly change during the day, so does the MPP. Thus, it is crucial that the MPP is always constantly tracked so that the MP can be obtained from the panel.

The solar irradiation has major impact on the P-V and I-V curves of a PV cell. An increase in irradiance causes a large positive effect on I_{sc} and small positive effect on V_{oc} , thus, increasing the power generation. The I_{sc} is directly proportional to the level of irradiance. The greater the solar irradiation, the greater the solar input to the PV cell, the higher photo-generated current, and hence the I_{sc} increases. The V_{oc} increases with an increase in solar irradiation. This is because the electrons are fed with higher excitation energy when more sunlight shines on the PV cell, thus increasing mobility of the electron and therefore generating greater power. Nevertheless, the irradiation effect on voltage is relatively small compared to the effect on the current. In summary, as the solar irradiation level increase, there is a big

positive current variation and small positive voltage variation. The effect of irradiance on PV panel is shown in Figure 1.3.

The temperature on PV panel also affects the P-V and I-V curves of a PV cell. The increase in temperature causes V_{oc} to decrease and I_{sc} to increase. The percentage of decrease in V_{oc} is larger than the increase in I_{sc} , which causes the reduction in the power generation. The influence of temperature on PV panel is shown in Figure 1.4.

2.6 Effects of Partial Shading on PV System

A PV panel is typically built using identical PV cells. It is common to have PSC effect on PV panel. Shading on PV panel occurs when there are clouds or trees that prevent the sunlight from reaching the PV panel. PSC happens when one or part of the PV module is shaded. This condition results in hot spots in the PV module, leading to a decrease in power generation.

In a series-connected PV module, if any of the PV cells in the module are shaded, the PV cells are forced to bear the same current as other cells which receive sufficient sunlight, thus, the shaded cells become reverse biased. At this condition, the shaded cell acts as load and dissipates power from other cells [18]. Rather than generating power, this shaded PV cell will start dissipating power leading to temperature rise, which can cause damage to the entire system. To prevent this, a bypass diode is connected in parallel to the PV cell. PSC causes multiple peaks in the P-V curve which complicates the tracking of MPP, as it has more than one local MPPs. The MP in a PSC is lower than that when there is no shading. It can be observed that one shaded PV cell causes large amount of power loss and the

efficiency of the PV system is low. Figure 2.6 (e) shows the PSC effect on PV output, in which multiple peaks are formed on the P-V curve.

With conventional MPPT, the tracking usually gets trapped at one of the local MPPs depending on the starting point of the D which affects the tracking efficiency. Several MPPT algorithms have been proposed to combat this issue. These newer MPPTs improve tracking by finding the global MPP instead of local MPP. Global MPP is the highest MPP formed in a multiple-peak P-V curve, whereas the local MPP is the remaining lower MPPs that is formed on the P-V curve due to PSC.

2.7 Non-Isolated DC-DC Converter in PV System

DC-DC converter in PV system has been widely used in present-day applications such as adapters and chargers [19-21], internet of things [22,23], motor controls [24], computer power supply, etc. The power supply to the load will vary unpredictably without any control if DC-DC converter is not used. Subsequently, the system can suffer significant damage from excess input power (P_{in}). A DC-DC converter plays a crucial role in aiding the MPPT to track the MPP. It is interfaced between the load and PV module and transfers MP from PV module to the load.

The PV system yields energy from the sun in various atmospheric conditions and supplies photovoltaic power (P_{pv}) in respect to voltage (V_{pv}) and current (I_{pv}) [4,5]. To achieve the desired output, the DC-DC converter takes V_{pv} and I_{pv} from the PV system and then regulates it by adjusting the D to balance the input and output load using MPPT.

There are different types of DC-DC converters used in a PV system. DC-DC converters can be grouped into two subclasses, isolated and non-isolated converters. Non-isolated converters are usually cheaper and simpler in design than the isolated

DC-DC converter [4]. Buck, boost and buck-boost are some conventional non-isolated DC-DC converters available. Buck-boost is produced when buck and boost converters cascaded together to overcome the drawbacks of buck and boost converters. Buck converter can only step down the output, whereas a boost converter can only step up the output. Ćuk, SEPIC and Zeta converters are buck-boost derived converters. Table 2.1 shows the summary of the available DC-DC converters used in PV system and its characteristics.

Table 2.1. Summary of types of DC-DC converters and its characteristics [25].

	Isolated DC-DC Converters	Non-Isolated DC-DC Converters
Converter	Fly Back, Forward, Resonant, Push Pull, Bridge	Buck, Boost, Buck-boost, Ćuk, SEPIC, Zeta, Luo, Resonant
Difference	Presence of an electrical barrier in between the inputs and outputs of the converter	Electrical barrier is not present
Barrier	High-frequency transformer	-
Advantage	<ol style="list-style-type: none"> 1. Employed in high voltage application such as grid system 2. Efficiently convert voltage with high ratio 3. Better noise filtering ability 	<ol style="list-style-type: none"> 1. Low-power grid & stand-alone system 2. Smaller & lighter 3. Lower cost

An efficient DC-DC converter maintains high P_{out} efficiency, a low P_{out} oscillation and quick tracking. A DC-DC converter makes up of inductor(s), capacitor(s), diode(s), and switch(es) which controls the D. Various variations of

DC-DC converter can be designed by modifying the component connections or configurations in the “switching network” and “low-pass filter” block in Figure 2.7.

The efficiency of a converter is worked-out using the Equation 2.5,

$$\eta_{\text{converter}} = \frac{V_{\text{out}} * I_{\text{out}}}{V_{\text{pv}} * I_{\text{pv}}} = \frac{(V_{\text{pv}} * I_{\text{pv}}) - P_{\text{losses}}}{V_{\text{pv}} * I_{\text{pv}}} \quad (2.5)$$

where V_{out} is the output voltage of the converter, I_{out} is the output current of the converter, V_{pv} is the output voltage of the PV panel, I_{pv} is the current output of the PV panel and P_{losses} is the losses in the converter. Extensive researches have been done on several types of converters. The following sections discuss briefly on selected literatures.

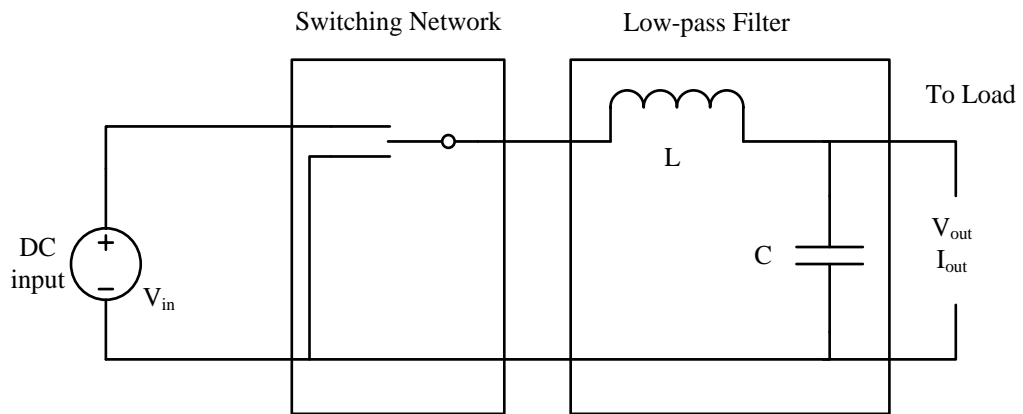


Figure 2.7 Basic model of a DC-DC converter.

2.7.1 Buck-boost Converter

Buck-boost converter is formed when buck and boost converter are cascaded. This converter can produce higher or lower V_{out} in comparison to the V_{in} , thus, making it suitable for a PV system, DC load, and battery input voltage. Buck-boost converter can track MPP over entire PV characteristic irrespective of the D value in which buck and boost converters unable to perform the tracking. This converter is less complex due to its number of components as only one inductor and one

capacitor are used. The cost of this converter is lower compared to SEPIC, Ćuk, and Zeta due to the number of components used.

The drawback of this converter is, it produces a high P_{out} oscillation. To overcome this, it needs great filter inductor and capacitor. Furthermore, the output polarity of the buck-boost converter is the opposite of the input polarity. This condition can be corrected by adding an isolation transformer into the circuits or by adding more switches, but unfortunately the cost and size of the converter also increase. This converter is also proven to be less efficient than other converter topologies [7,9]. To overcome these drawbacks, some derivations are made onto its circuitry, and new converters were formed; i.e. Ćuk, SEPIC and Zeta. Figure 2.8 shows the buck-boost converter configuration.

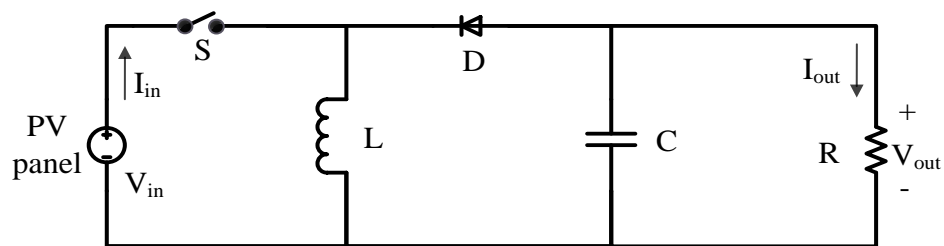


Figure 2.8 Circuit configuration of buck-boost converter.

At ON state (switch is closed), there is a short circuit at the switch and open circuit at the diode since it is reversed biased. The current from the source will flow into the inductor, and its energy will rise. At this time, the load receives continuous current from the capacitor. At OFF state (switch is open), there is an open circuit at the switch and short circuit at the diode since it is forward biased. The energy will be discharged from the inductor, and the current will flow to the load and capacitor through the diode [9]. The V_{out} of this converter can be higher or lower than the input voltage (V_{in}) depending on the D value of the converter. The relationship between

the V_{out} , V_{in} , output current (I_{out}), input current (I_{in}), output impedance (R_{out}), and input impedance (R_{in}) are shown in Equation 2.6, Equation 2.7 and Equation 2.8.

$$\frac{V_{out}}{V_{in}} = -\frac{D}{1-D} \quad (2.6)$$

$$\frac{I_{out}}{I_{in}} = -\frac{1-D}{D} \quad (2.7)$$

$$\frac{R_{in}}{R_{out}} = \left(\frac{1-D}{D}\right)^2 \quad (2.8)$$

Buck-boost commonly yields higher performance than buck and boost converter. An interleaved buck-boost converter with magnetically coupled inductor is designed by employing PO MPPT. The converter's effectiveness and output power were greater than conventional buck-boost converter [26]. A control algorithm is proposed to improve the light-load performance of 3.19 % by regulating the inductor current oscillation. Thus, a condition in the current operation determines the inductor core loss. The effectiveness of this algorithm was 97.7 % and can be applied in most non-inverting synchronous buck-boost converters [27].

The following research focused to reduce the cost and quantity of components applied in the system. A two-switch buck-boost DC-DC converter that uses piecewise linear approach was introduced to execute the system in a low-cost 8-bit micro-controller. The proposed system demonstrates the efficiency and practical application of a PV emulator [28]. On the other hand, a four-switch buck-boost converter that operates under continuous conduction mode (CCM) using PO is produced. The benefit of this approach is the non-inverted V_{out} and decreased passive components quantity [29]. A single-switch voltage equalizer that uses a multi-stacked buck-boost converter is proposed to function in PSC. The system can be formed by fusing capacitor–inductor–diode filters on conventional buck-boost converters. The approach was straightforward and could harvest MP better, thus

improving its effectiveness. Local MPPs in the P-V curve were removed by using an equalizer [30].

A multi-input single-output DC-DC converter that is made of many buck-boost converters and enclosed with one conventional boost converter is proposed. The approach decreased the current stress, providing no boundary in regulating D and maintained a broad input range. The approach could also work if one or more inputs break down. High voltage gain and variable control were some other advantage of the approach [31]. An FL controller integrated DC-DC buck-boost converter is proposed for the PV system. A microcontroller was applied to determine the V_{in} and V_{out} . FL controller regulates the charging circuit, and a microcontroller watches the state of charge of the battery [32].

2.7.2 Ćuk Converter

Similar to buck-boost converter, Ćuk converter is able track over all I-V curve regions and gives inverted V_{out} polarity. The difference between a buck-boost and Ćuk converter are, Ćuk converter uses an extra inductor and capacitor to store energy and transfer power. Figure 2.9 shows the Ćuk converter circuit configuration. At ON state, the diode is opened, and the switch is shorted. The current in the inductor 1 increases linearly and capacitor 1 transfers its energy to inductor 2 and capacitor 2. At OFF state, the diode is forward biased, and it carries the current from inductor 1 and inductor 2 and transfers to capacitor 1 and capacitor 2 respectively. This results in a reduction of inductors current value [9]. The V_{out} , V_{in} , I_{out} , I_{in} , R_{out} , R_{in} equations of Ćuk converter are similar to Equation 2.6, Equation 2.7 and Equation 2.8 respectively. The complexity of this converter is high. The drawback of Ćuk converter is it has high I_{out} oscillation.